1 Research background and Fundamentals

1.1 Radiotherapy

Since the discovery of X-rays in 1895 the radiation has been used by physicans for treating patients. In the begining only superfical diseases could be cured, but as time and technology progressed X-ray tubes gained on voltage and allowing treatment of deeper suited tumors.

The radiation from linear accelerator was first used in medicine in 1953. Because the beam is more collimated and energies are higher than X-ray tube the cure rates improved tremendously. The next big milestone was introduction of computeres in the field of radiotherapy. This led to better diagnostic tools, such as computed tomography scans (CT), magnetic resonance imaging (MRI) and positron emission tomography (PET). With those tools the location of the tumor could be much better estimated and hence the physicans could easier prescribe treatment. The potential of computers were afterwards exploited also in treatment planning with intensity modulated radiation therapy (IMRT) which, together with diagnostic tools, provides an exact dose shaping in accordance to patient specific tumors.

In 1946 it was discovered that protons could be used alongside photons for cancer treatment. Furthermore it was shown that protons have preferable depth dose profile compared to photons. First patient treatment soon followed in the early 1950's at Lawrence Berkeley Laboratory, USA. Heavier ions, such as He^{2+}, ^{20}Ne and ^{6}C were also used later on for treatment. In the begining only passive beam delivery was used for treatment and in the 1990's active beam solutions were developed at Paul Scherrer Institut (PSI), Villigen (Switzerland) for protons and at GSI, Darmstadt (Germany) for carbon ions.

Both treatment modalities (photons and ions) use the same principle to eliminate cancer cells. The physical and biological mechanism behind it will be explained in detail in the following sections.

1.2 Physcial and biological basics of radiotherapy

1.2.1 Interaction of radiation with matter

The interactions between photons and ions with matter are quite different, as can be seen from depth dose distributions in Figure 1.1. Photons deposit highest local dose shortly after entering

the matter (at the energies used in radiotherapy). Ions deposit most of their dose right before they stop in the Bragg Peak region. The position of the Bragg Peak depends on the energy of the ions, which is exploited in the treatment of deep suited tumors.

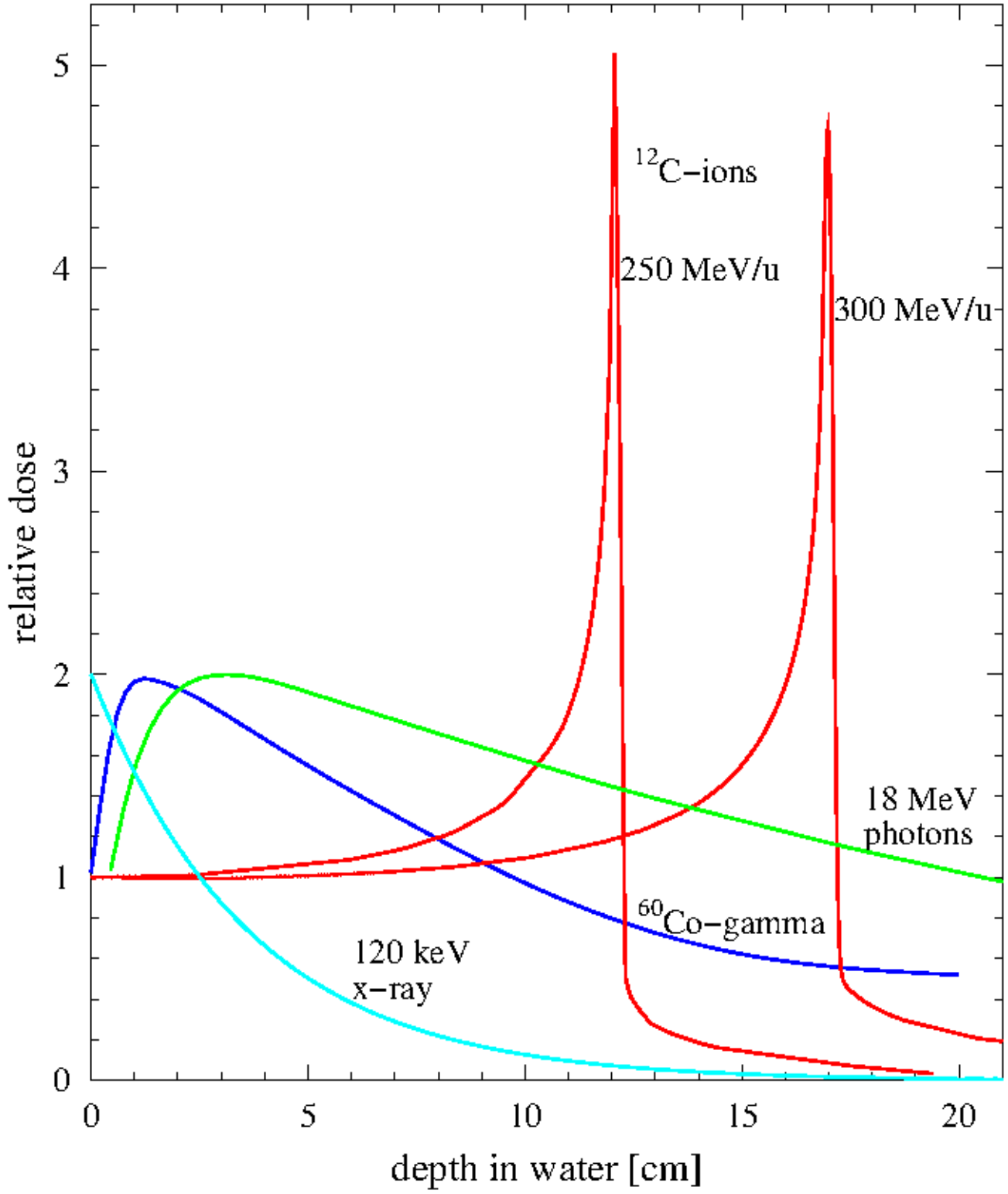

Figure 1.1: Photon and carbon ions depth dose distributions at different energies. Photons start with a build up, which is followed by an exponential decrease after. Ions deposit most of the dose at the end of the particle track, the Bragg peak. Figure taken from [Schardt et al., 2010]

1.2.2 Dose definition

Physicis in radiotherapy revolves around dose, D, which is defined as the ratio of the absorbed energy dE per mass element dm [ICRU, 1993]:

$$D = \frac{dE}{dm} \tag{1.1}$$

Usually we can describe energy loss of a beam in a thin layer of material, dE/dx. Dose can be then rewritten as:

$$D = \frac{dE}{dx} \times \frac{1}{F} \times \frac{1}{\rho} \tag{1.2}$$

where F is fluence and ρ the material denisty.

Interaction of photons with matter

Photons mostly interact with matter in one of the following ways: coherent or Rayleigh scattering, photoelectric effect, Compton scattering and pair production. The cross section, σ, for each of these processes depends as well on the energy of the indicent photons as on the atomic number of the absorbin material [Lilley, 2006]. The decreasing photon intesity in matter, I, can be described as:

$$I = I_0 \cdot e^{-N\sigma x} = I_0 \cdot e^{-\mu x} \tag{1.3}$$

where I_0 stands for the initial intensity of the photons, x the depth of the material in units of length, N the atomic density of the material and μ is the attenuation coefficient. The cross section, $sigma$ is the sum of all possibile Interaction processes.

$$\sigma = \sigma_{rayleigh} + \sigma_{photoelectric} + Z\sigma_{compton} + \sigma_{pairproduction} \tag{1.4}$$

The energy range of photons used in radiotherapy is between 100 keV and 25 MeV. The dominating process in this energy range is Compton scattering [Alpen, 1998]. The electrons resulting from Compton interaction scatter mostly in a forward direction. Therefore a maximum of the depth-dose profile occurs when electons stop at a certain depth, the mean electron range. After this build up the dose deposition decreases exponentially (see Figure 1.1 and eq. 1.3).

Interaction of ions with matter

Ions can interact with matter either with elastic columb scattering from target nuclei (nuclear stopping) or with inelastic collision with target electorns (electronic stopping). At the ion energies used in radiotherapy, which are less then 500MeV/u, the electronic stoping is the dominated interaction. This results in ionization and excitation of the atoms in target.

The mean rate of ions energy loss in matter is described by the Bethe-Bloch formula [Bethe, 1930, Bloch, 1933]. Since we are interested in low ion energies, we can make the following approximation:

$$-\left\langle \frac{dE}{dx} \right\rangle = \frac{4\pi N_e z_{eff}^2}{m_e v^2} \left(\frac{e^2}{4\pi\epsilon_0} \right)^2 \left[ln\left(\frac{2m_e v^2}{I} \right) + correction \right] \tag{1.5}$$

here N_e is the materials electron density, e and m_e are the charge and mass of an electron, ϵ_0 the electrical field constant and I the mean excitation energy of the absorber material. Barkas formula [Barkas, 1963] can be used for the approximation of the effective projectile charge z_{eff}:

$$z_{eff} = z\left(1 - e^{-125\beta z^{\frac{2}{3}}}\right) \tag{1.6}$$

where β is the projectile speed in units of c.

The energy loss of ions is proportional to z_{eff} and inversely proportional to v^2. The shape of the curve in Figure 1.1 can now be understood. Ions enter the matter with a high velocity, resulting in a small energy deposition. Their velocity gradualy decreases, which in turn increases the energy deposition. The maximum of the energy loss is called Bragg peak or particle range.

Lateral scattering and range straggling of ions

As mentioned in section 1.2.2 ions interact mostly via electronic stopping at energies used in radiotherapy. However, nuclear stopping still occurs and it is the main reason for lateral scattering. The angular spread of ions is dependent on the mass of the target nuclei and on the momentum of the indecient ions [Molière, 1948]. The lateral scattering is proportional to mass of the target nuclei and inversely proportional on the momentum of indecient ions. Carbon ions have thus less lateral scatter then protons. Experiments have shown that carbon ions have three times smaller angular spread compared to protons at the same range in water (15.6 cm, 150 MeV/u protons and 285 MeV/u ^{12}C ions) [Schardt et al., 2010].

Statistical fluctuations of specific electronic stopping events cause range straggling of ions. If the number of collisions is high or the material is thick enoguh these fluctuations can be

approximated by a Gaussian probability distribution [Bohr, 1940, Ahlen, 1980]. The straggling width σ_R is proportional to:

$$\sigma_R \propto R/\sqrt{M} \tag{1.7}$$

where R is the mean range of ions and M the ion mass. Thus, the heavier the ion is, the less range straggling it has. Carbon ions have 3.5 smaller range straggling when compared to protons [Schardt et al., 2010].

Nuclear fragmentation

When transversing through matter ions (except protons) can be fragmented into ions with lower Z. The lower Z fragments travel in the same direction as projectile ions and have a significant contribution to the dose deposited (see Figure 1.2). It is essential that this fragments are included in the treatment planning, so that the accurate dose can be assesed.

After colliding with target projectile fragments enter in a excited state. De-excitation occurs through emisson of nucleons, nucleon clusters and photons. Two of the possible fragments of projectile ^{12}C ions are isotopes ^{11}C and ^{10}C, which are both β^+ emmiters [Kraft, 2000]. The resulting positron is annihilated with electrons in matter, resulting in two photons traveling in opposite direction. This can be used in PET (Positron Emission Tomography) without exposing patient to additional radiation..

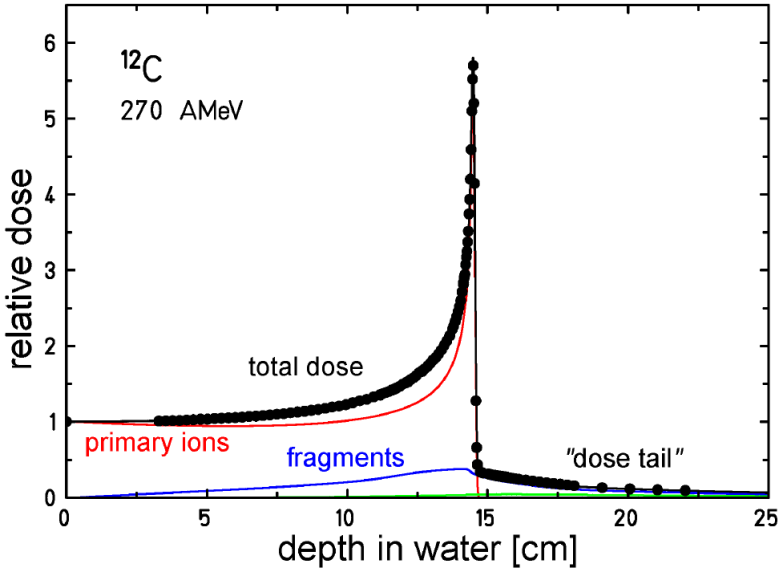

Figure 1.2: Impact of fragmantation on a depth dose distribution of carbon ions. Main contribution to the overall deposited dose (black line) comes from the primary ions (red line). The produced fragments (blue line) have a smaller impact, but non-negleigble especially in the dose tail behind the Bragg peak. Figure taken from [Groezinger, 2004]

As mentioned in section 1.2.2 ions used in radiotherapy lose most of their energy via inelastic Coulumb scattering on target electrons. Such electrons can be libirated from target atoms and are called secondary electrons, also δ-electrons. δ-electrons also travel throguh matter, further scattering and may even cause secondary ionization of the target atoms. When δ-electons energies are larger than >50 eV, ionization becomes dominant process, which produces a large number of additional electons [Kraft, 2000, Schardt et al., 2010].

The radial dose profile and track diameter is defined by the energy spectrum of the δ-electrons. Most of the δ-electorns are concentrated around the projectile ions path, since they receive small energy transfers or are scattered in the direction of indicent ions. Different models [**?**], Monte Carlo simulations [**?**] predict radial dose fall-off approximatelly with $1/r^2$ for radial distances r. Varma et. al. have confirmed this experimentaly [Varma et al., 1977]. The maximum radial distance r_{max} is defined by the most energetic δ-electrons, which are related to energy, E, of the projectile ions [Kiefer and Straaten, 1986].

$$r_{max} = E^{1.7} \tag{1.8}$$

Following equation 1.5, E is corelated to Z^2 and $1/\beta^2$, which means track structure is highly dependent on the projectile ion species and energy. This is well demonstrated on Figure 1.3: Carbon ions have much more dense ionization structure compared to protons [**?**]. δ-electrons have low energies, and thus the r is on nanometer scale. As the energy of projectile ions decreases, their stopping power increases and causes significantly larger number of δ-electorns. The energy deposited by δ-electrons in medium is described using the Linear Energy Transfer (LET), which is closely related to dE/dx. Fast ions, with little ionization, have thus small LET, while slow ions, with large ionization, have a high LET.

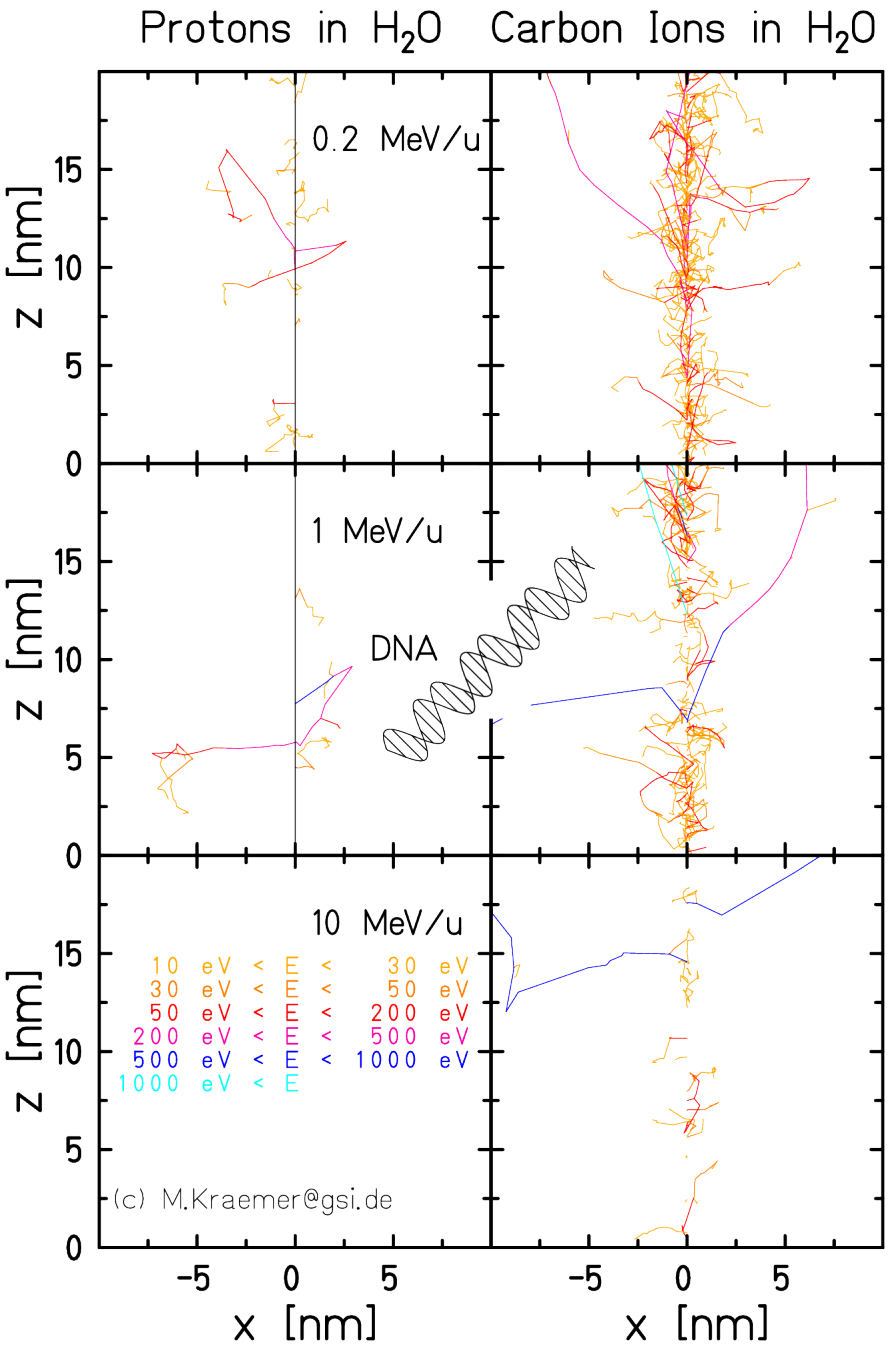

Figure 1.3: Microscopic track structure of protons (left side) and carbon ions (right side) at different energies. Protons and high energy carbon ions are low LET radiation and hence sparsely ionizing. Low energy carbon ions on the other hand are high LET radiation and hence densely ionizing. For comparison the size of the DNA is displayed. Figure courtesy of Michael Krämer.

Bibliography

[Ahlen, 1980] Ahlen, S. (1980). Theoretical and experimental aspects of the enery loss of relativistic heavily ionizing particles. *Rev. Mod. Phys.*, 52(1):121.

[Alpen, 1998] Alpen, E. L. (1998). *Radiation Biophysics*. Academic Press, California, USA, 2nd edition edition.

[Barkas, 1963] Barkas, H. (1963). *Nuclear Research Emulsions*, volume 1. Academic Press, New York, USA and London, UK.

[Bethe, 1930] Bethe, H. (1930). Zur Theorie des Durchgangs schneller Korpuskularstrahlung durch Materie. *Annalen der Physik*, 5(5):325–400.

[Bloch, 1933] Bloch, F. (1933). Zur Bremsung rasch bewegter Teilchen beim Durchgang durch Materie. *Annalen der Physik*, 5(16):285–321.

[Bohr, 1940] Bohr, N. (1940). Scattering and stopping of fission fragments. *Phys . Rev.*, 58(7):654 – 655.

[Groezinger, 2004] Groezinger, S. O. (2004). *Volume Conformal Irradiation of Moving Target Volumes with Scanned Ion Beams*. Thesis/dissertation, TU Darmstadt.

[ICRU, 1993] ICRU (1993). Report 50. Report.

[Kiefer and Straaten, 1986] Kiefer, J. and Straaten, H. (1986). A model of ion track structure based on classical collision dynamics. *Phys. Med. Biol.*, 31(11):1201–1209.

[Kraft, 2000] Kraft, G. (2000). Tumor therapy with heavy charged particles. *Progress in Particle and Nuclear Physics*, 45(Supplement 2):S473–S544.

[Lilley, 2006] Lilley, J. (2006). *Nuclear Physics - Principles and Applications*. Wiley, Manchester, UK.

[Molière, 1948] Molière, G. (1948). Theorie der streuung schneller geladener teilchen ii, mehrfach- und vielfachstreuung. *Zeitschrift für Naturforschung*, 3a:78–97.

[Schardt et al., 2010] Schardt, D., Elsaesser, T., and Schulz-Ertner, D. (2010). Heavy-ion tumor therapy: Physical and radiobiological benefits. *Rev. Mod. Phys.*, 82(1):383.

[Varma et al., 1977] Varma, M. N., Baum, J. W., and Kuehner, A. V. (1977). Radial dose, LET, and W for 160 ions in N2 and tissue-equivalent gases. *Radiat. Res.*, 70(3):511–518.